



Synthesis of Peculiar Structure of Hydroxyapatite Nanorods by Hydrothermal Condition for Biomedical Applications

Saheb Ali Manafi^a, Sareh Khani, Atefeh Soltanmoradi

^aDepartment of Ceramics, Shahrood Branch Islamic Azad University, Shahrood Iran

Abstract

In the present work, the effect of $\text{Ca}(\text{NO}_3)_2 \cdot 4\text{H}_2\text{O}$ and $(\text{NH}_4)_2\text{HPO}_4$ primary solutions as the beginning materials in synthesis of a calcium phosphate phase, was examined. So, we investigated the wet chemical reactions in solution at different temperatures by a hydrothermal condition aimed at hydroxyapatite ($\text{Ca}_{10}(\text{PO}_4)_6(\text{OH})_2$); (HAp) synthesis. The powders were investigated by XRD, SEM, FE-TEM, HRTEM, EDAX, SAED and FT-IR. It was found that HAp has a length of approximately several micrometres and a diameter of 20-30 nm with different morphologies. As a matter of fact, the method of hydrothermal method guarantees the production of HAs for different applications especially clinical applications.

Keywords: Biomedical Engineering; Hydroxyapatite; Nanorod; Osseoconductive.
Received: October 1, 2010; *Accepted:* December 6, 2010

1. Introduction

Hydroxyapatite (HA) coatings are used as material for metal implant coatings where they provide strong fixation of implant and bone and minimize adverse foreign body reaction of organism. HA coating acts as barrier between metal and medium hindering poisoning of organism with metal ions. Interaction of HA with organism depends on its chemical composition, size and morphology of crystals. Transfer from micro- to nanostructured materials allows to strengthen biological activity, to control resorption kinetics, to improve mechanical properties.

The main problem of application of ceramics coating on metals is insufficient adhesion with substrate. This problem can be solved by use of HA-polymer composite materials. This work proposes composite calcium phosphate chitosan (Ca-P/Ch) coating applied with electrochemical deposition method. Chitosan is natural biopolymer and has a complete biocompatibility with organism tissues that allows to use it in various fields of medicine [1, 2]. The main characteristic of artificial synthetic calcium phosphates (CaP), for which they are preferred in studies and applications concerning biomedical bone-substitute thin films deposition, is their innate similarity with the mineral compounds from bone and teeth, which represents the basis of osseoconductive behaviour [3,4]. Hydroxyapatite (HA)

*Corresponding author: Saheb Ali Manafi,
Shahrood Branch Islamic Azad University, P.O.Box 36155-163,
Shahrood Iran
Tel: (+98)2733334530, Fax: (+98)2733334537
E-mail: ali_manafi2005@yahoo.com

$\text{Ca}_{10}(\text{PO}_4)_6(\text{OH})_2$ presents the biggest stability of all calcium phosphates, being the less soluble in physiological conditions in the following series of relative solubility values (MCP>TTCP> α -TCP>DCPD>DCP>OCP> β -TCP>CDHA>HA)[1,5]. Therefore, synthesis of nanoscale hydroxyapatites will largely improve their clinical applications. In the present work, the hydrothermal technique was developed for the formation of ultra-high crystalline hydroxyapatite nanorods. The nanorods are interestingly crystallized and single crystal with hexagonal heads. These high-quality hydroxyapatite nanorods represent well-defined nanoscale structure needed for both fundamental studies and clinical applications.

2. Experimental procedures

All of the reactants, $\text{Ca}(\text{NO}_3)_2$ (99% MERCK), $(\text{NH}_4)_2\text{HPO}_4$ (99% Alfa), and NaOH (96% Aldrich), were of reagent grade and used without further purification. In a typical experiment, an alkali solution, cetyltrimethylammonium bromide ($(\text{C}_2\text{H}_5)_3\text{N}^+(\text{C}_2\text{H}_5)_3\text{Br}^-$, CTAB)/ $\text{Ca}(\text{NO}_3)_2$ /NaOH/ $(\text{NH}_4)_2\text{HPO}_4$ and distilled water, was selected for this study. As a typical synthesis, two identical solution were prepared by dissolving CTAB (2 g) in

50 ml (0.2 M, 2.36 g) of $\text{Ca}(\text{NO}_3)_2$ and 50 ml (0.12 M, 0.79 g) of $(\text{NH}_4)_2\text{HPO}_4$. The mixing solution was stirred for 30 min. until it became transparent. Next, 2 ml of 1 M NaOH aqueous solution and 10 ml of distilled water were added to the solution, respectively. After substantial stirring, the two optically transparent alkali solutions were mixed and stirred for another 30 min. The resulting alkali solution was then transferred into a 30 ml stainless Teflon-lined autoclave and was heated at 150 °C for 18 h. The resulting suspension was cooled to room temperature right after the heating and was then stored at a constant temperature of 50 °C. After 18 h, samples were collected and washed several times with distilled water and then deionized water. For these experiments, a Siemens D500 powder diffractometer with the $\text{K}\alpha_1$ radiation of copper ($\lambda = 1.5406 \text{ \AA}$), was used and X-ray diffraction patterns were recorded in an angular range of $2\theta = 20\text{--}60^\circ$. The obtained HAp nanorods were characterized with scanning electron microscopy, energy-dispersive X-ray spectroscopy (SEM/EDX, XL30). The powder product was further investigated using Fourier transform infrared (FTIR) spectroscopy in a Bruker-IR spectrometer from 500 to 4000 cm^{-1} using the KBr technique and operating in the transmittance mode. The size distribution and

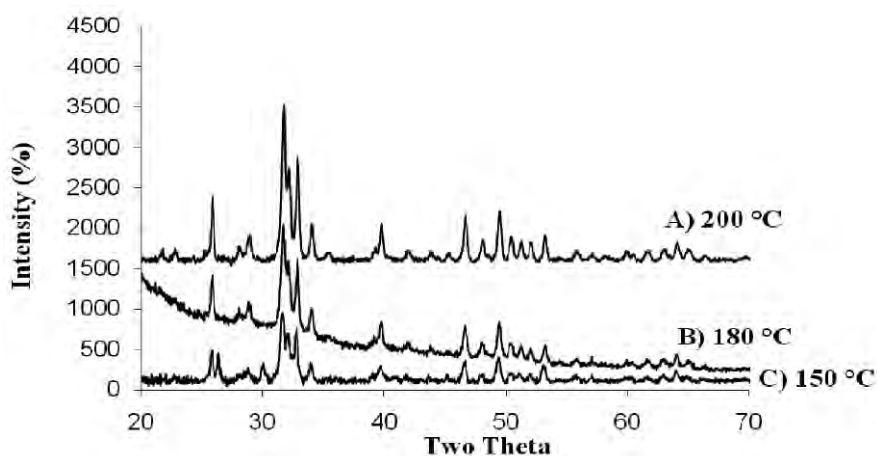


Figure 1. XRD patterns of HAp samples at different temperatures (A) 150 °C, (B) 180 °C and (C) 200 °C.

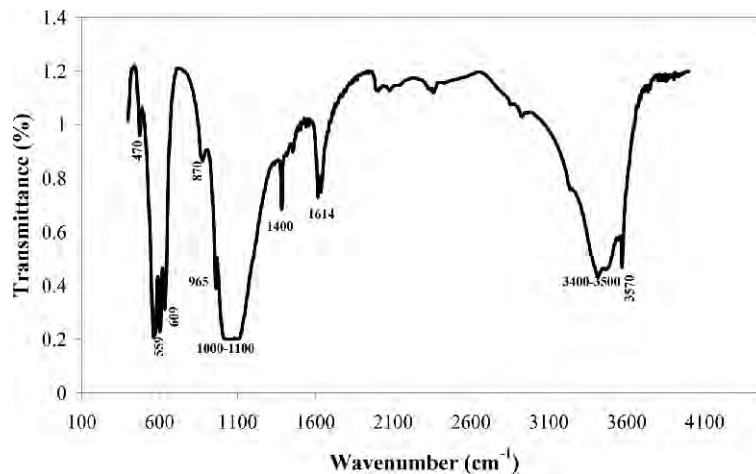


Figure 2. The FTIR spectrum of the HAp nanorods.

morphology of the samples were analyzed by field emission gun (FEG) transmission electron microscope (TEM), selected area electron diffraction (SAED) observation on a Philips CM200 transmission electron microscope operated at 200 kV.

3. Results and discussion

The XRD patterns in Figure 1 show that the as-synthesized HAp samples at different temperatures (150, 180 and 200 °C) for 18 h are the hexagonal phase with cell constants very close to the values in the literature [6]. All peaks of the products can be indexed to stoichiometric HAp composition with hexagonal structure. No tri-calcium phosphate (TCP) and other impurity phases are detected. The strong and sharp peaks and very low

backgrounds reveal that the as-synthesized HAp nanoparticles had a high degree of crystallinity. The broadening of the diffraction peaks indicates that the samples are nanosize. Full width at half-maximum (FWHM) increases with the increase of autoclave temperature, which indicates that the sizes of the products increase with the increase in the high temperature. Nanoparticles generated following 30, 60, and 90 nm residence sizes of approximately 25, 30, and 50 nm, respectively. These were calculated from the half-width of the peaks of the XRD patterns, using the Scherrer formula [7].

The shape of the strong diffraction peaks indicates that the samples are fairly well high crystallized. The crystallinity of HAp powders

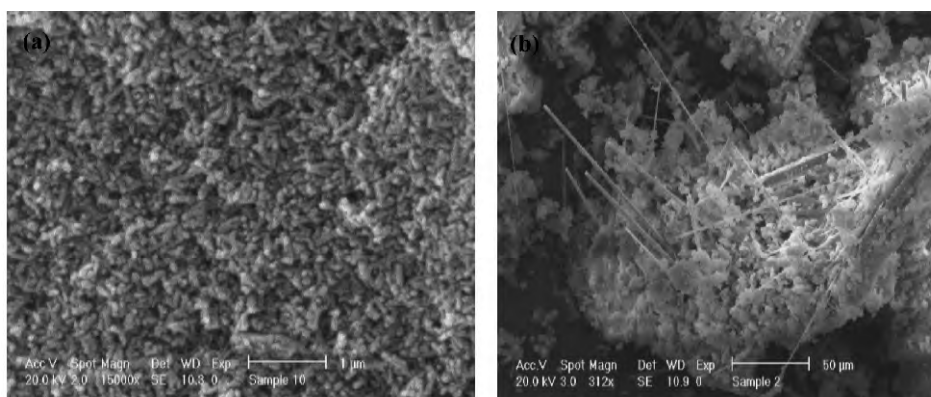


Figure 3. SEM images of (a) as-synthesized HAp obtained at hydrothermal condition and (b) high aspect ratio nanorods.

synthesized via hydrothermal method was much higher than those synthesized via other methods. The XRD results showed that the bioceramics were composed of highly crystalline and single phase HAp, and no obvious impurity phase could be found. The shape of the diffraction peaks suggests that the sample could be well crystallized. The broadened nature of these diffraction peaks implies that the grain sizes of sample are nanometer scale. Estimating from the Debye-Scherrer formula, the average grain size is 20 ± 10 nm.

FTIR analysis revealed the presence of carbon on the surface of the HAp. Figure 2 shows the transmittance infrared spectrum of synthetic HAp in the $4000\text{-}650\text{ cm}^{-1}$ region. A narrow band located near 965 cm^{-1} (962 cm^{-1} in Figure 2) represents the ν_1 mode of PO_4^{3-} ions in apatite. The main signal of phosphate appears in the triply degenerate ν_3 domain ($1000\text{-}1100\text{ cm}^{-1}$). The adsorption band at 3570 cm^{-1} confirmed the presence of

OH- groups. The ν_2 peak of CO_3^{2-} is located at 870 cm^{-1} , this absorption results from out-of-plane stretching. The ν_3 mode, near 1400 cm^{-1} , is the strongest IR peak for carbonate. This peak is actually composed of two bands (1454 and 1421 cm^{-1} , in Figure 2) [8, 9]. The shape of the ν_3 signal and the absence of the C-O absorption bands at 710 cm^{-1} indicate that no calcite was associated with the HAp. Carbonate ions can substitute for either OH- or PO_4^{3-} ions in the apatite structure (type A CO_3^{2-} or type B CO_3^{2-}) [10, 11]. The FTIR results further confirm that the as-synthesized powders are pure HAp.

Figure 3a is the scanning electron microscopy (SEM) image of the as-synthesized HAp obtained at hydrothermal condition, which displays nanorods with excellent uniformity. In Figure 3b, the as-synthesized HAp sample shows a typical outstanding morphology, high ordered nanorod structure and high aspect ratio.

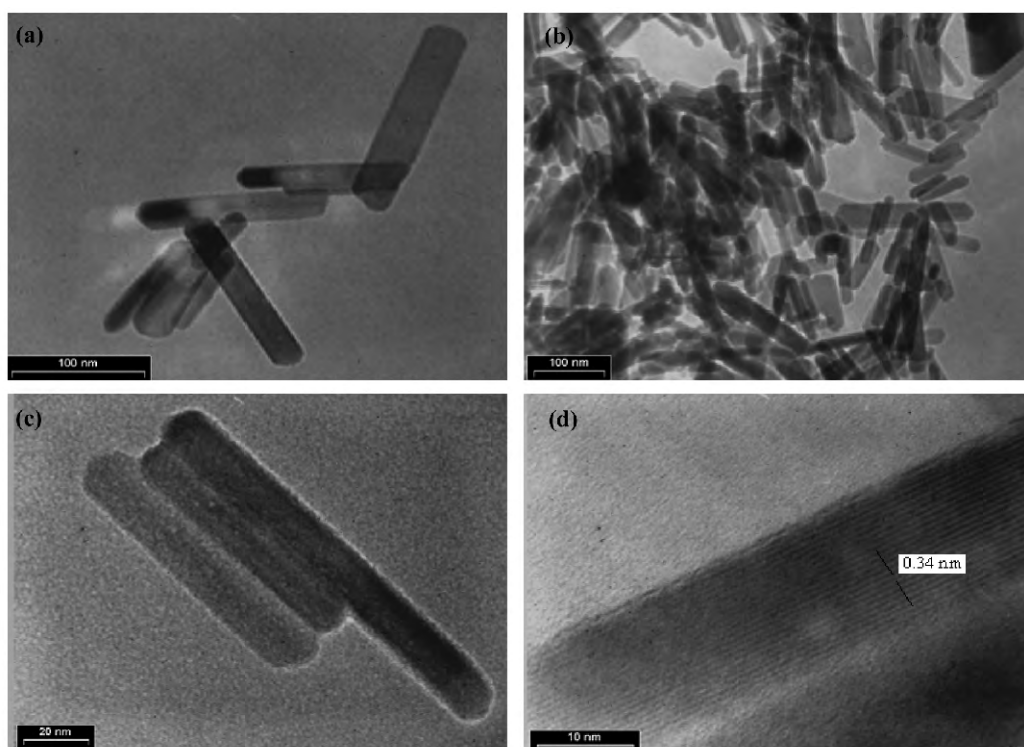


Figure 4. TEM images of (a) single crystal nanostuctures; (b) high yield efficiency; (c) ultrahigh crystallinity; (d) HRTEM.

A field emission gun (FEG) CM200 high resolution transmission electron microscope (HRTEM) was used to characterize the HAp nanorods and HAp single crystals, and typical TEM are shown in Figure 4. Figure 4a clearly shows that the product consists of single crystal nanostructures 20 ± 10 nm in diameter and about 80 ± 20 μm in length, which are "sub-60 nm HAp nanorods" in this paper. The yield of the prepared nanorod hydroxyapatite estimated by TEM observations is about 99.9 % relative to the samples on copper grids, and the much less contents of the obtained product are nanoparticles (Figure 4b). Thus, the high yield efficiency of this approach for the synthesis of HAp can be concluded, with a ultrahigh crystallinity (Figure 4c) and an excellent yield rather than previous works. In further investigation, the HAp nanorods were analyzed by HRTEM in detail, and all nanoparticles showed uniform lattice fringes, meaning that no amorphous product was formed. Figure 4d is the HRTEM image of a single crystal HAp nanorod, which clearly indicates that the HAp nanorod is structurally uniform single crystalline with ultra-high crystallinity. The interplanar spacing values are calculated from Bragg's diffraction equation using the diffraction ring diameter and the camera length of the transmission electron microscope. The calculated results indicate the fringe spacing about 0.34 nm

observed in Figure 4d agrees with the separation between the (002) lattice planes of hexagonal phase and nanorods have grown in a [001] direction. The EDS spectrum of the nanorod shows that these are only elemental O, Ca and P except the elements of C and Cu, which come from the supported grid for TEM measurement. The atomic ratio of Ca to P according to EDS semi-quantitative assessment is about 1.67, which was equal to the theoretical value. Those results are in good agreement with the results of ICP.

After all, peculiar results in present work were shown in selected areas of electron diffraction (SAED) pattern. Figure 5 shows the evolution of SAED pattern obtained using a small aperture size in order to ensure that the cross sectional area examined, belonged to a selected small region of single crystal and was ca. 0.1 μm in size. This was also done to prevent contribution from the streak and ring distortions of the ED patterns arising from the expected mosaicity of the sample.

SAED observations was performed in the long-axis of the HAp nanorod. The diffraction pattern from area A showed clear spot (Figure 5a) corresponding to an apatite structure with high crystallinity. So, all diffraction patterns from the long-axis of the same nanorod sample showed the same geometry, it was concluded that the apatite fibers preferentially grow along the c-axis to develop the a(b)-plane of hexagonal HAp. The patterns

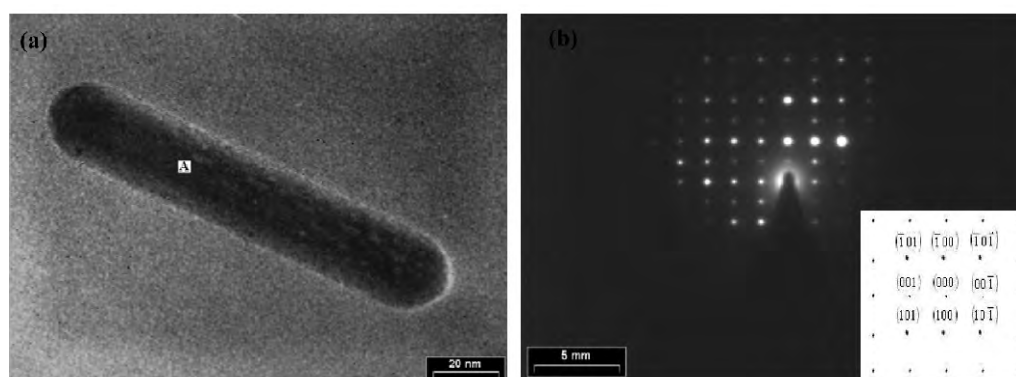


Figure 5. (a) Individual HAp nanorod (b) A single nanorod selected for undertaking intensive characterization by SAED

obtained were indexed to the hexagonal lattice of hydroxyapatite viewed along the $\langle 110 \rangle$ zone, and the flat surface is (110) (the lower right insert in Figure 5b).

At the same time, SAED patterns of the samples were consistent with the ultra-high crystallinity, and the diffraction spot could be indexed as the hexagonal phase. This result was in good agreement with the result of XRD.

4. Conclusion

In summary, an effective method was developed for the formation of ultra-crystallinity rod-like HAp. The nano-rods are highly high aspect-ratio, high-crystalline and uniformly structured. These high-quality HAp nano-rods represent well-defined nanoscale structure needed for both fundamental studies and clinical applications. As the matter of fact, hydrothermal method guarantees its production in the synthesis of HAp for clinical applications.

References

- [1] Layrolle P, Daculsi G, in: B. Leon, J.A. Jansen (Eds.), *Thin Calcium Phosphate Coatings for Medical Implants*, Springer, 2009, pp. 10-2.
- [2] Lake PA, Morin MA, Pitts FW, J. *TOPIC Neurosurg J.* 1970; 32: 597-602.
- [3] Elliott JC. *Structure and chemistry of the apatites and other calcium orthophosphates*, Elsevier, Amsterdam, 1994.
- [4] Suchanek W, Yoshimura M. *TOPIC J. Mater. Res.* 13 (1) (1998) 94-117.
- [5] Leon B, Jansen JA. *Thin calcium phosphate coatings for medical implants*. Springer, 2009, pp. 101-155, pp. 175-98.
- [6] Komlev VS, Barinov SM, Koplík EV. *TOPIC Biomaterials* 23, 3449 (2002).
- [7] Jenkins R, Snyder RL. *Introduction to X-ray powder diffractometry*, John Wiley & Sons, New York (1996).
- [8] Doi Y, Moriwaki Y, Aoba T, Takahashi J, Joshin K. *TOPIC Calcif. Tissue Int.* 34, 178 (1982).
- [9] Reigner P, Lasaga AC, Berner RA, Han OH, Zilm KW. *TOPIC Am. Mineral.* 79, 809 (1994).
- [10] Elliot IC, Ph.D. Thesis, University of London, London, England (1964).
- [11] Bonel GA. *TOPIC Ann. Chim.* 7, 65 (1972).